

Nonlinear Regression Analysis for Side Resistance of Socketed Piles in Rock Formations of Dubai Area

Mohammad Yamin · Zahid Khan · Hesham El Naggar · Nasser Al Hai

Received: 12 January 2017 / Accepted: 22 May 2018 / Published online: 26 May 2018
© Springer International Publishing AG, part of Springer Nature 2018

Abstract Pile capacity installed in Dubai rock formation is calculated based primarily on socket shaft resistance. During preliminary design, socket resistance is estimated by using correlations with rock strength that do not reflect the behavior of Dubai rock formations as well as construction practices. Consequently, large discrepancy is often noticed between predicted pile capacity and that determined from the results of pile load tests. In this study, a new predictive model is developed for socket shaft resistance of piles constructed in rock formations of Dubai area. Five (5) instrumented piles of different diameters and socket lengths ranging from 10 to 15 m are tested. The proposed model takes into account the compressive strength of the rock in addition to the pile movement at

the top of socket to predict its side resistance. The average side resistance of the socket predicted using the proposed model compared well with the results of load transfer along the sockets of the test piles. In addition, the developed model is compared with published models from other regions to illustrate the area specific nature of correlations and factors that affect their generality are highlighted.

Keywords Socketed piles · Side resistance · Rock mass strength · Non-linear model

1 Introduction

Piles are usually used to support mid to high rise structures in the United Arab Emirates (UAE). The piles in Dubai area of UAE are designed as socketed piles, where their capacity is derived from the side resistance of the rock Socket. These piles are constructed with Socket lengths considerably larger than their diameter to provide the required compressive capacity as well as uplift resistance. The end bearing resistance is neglected due to its limited mobilization at serviceability limit state. In the preliminary design stage, the side resistance is estimated from empirical correlations with unconfined compressive strength (σ_c) of the intact rock and other rock mass/interface properties (e.g. Rosenberg and Journeaux 1976; Williams and Pells 1981; Rowe and Armitage 1987;

M. Yamin
Civil Engineering Department, Minnesota State
University, Mankato, USA
e-mail: mohammad.yamin@mnsu.edu

Z. Khan (✉)
Civil Engineering Department, American University of
Sharjah, P.O. Box 26666, Sharjah, UAE
e-mail: zhkhan@aus.edu

H. El Naggar
Civil Engineering Department, Western University,
London, Canada
e-mail: naggar@uwo.ca

N. Al Hai
DEC (Dynamic Engineering Consultants), Dubai, UAE
e-mail: nasser.alhai@decengineering.net

Kulhawy and Phoon 1993; Omer et al. 2003; Bouafia 2003; Kulhawy et al. 2005). The general form for the empirical correlation to estimate the maximum/limiting side resistance (f_{\max}) (in MPa) can be expressed as:

$$f_{\max} = A \times (\sigma_c)^B \quad (1)$$

where A and B are constants ranging from 0.2 to 0.8 and 0.159 to 1, respectively, and σ_c is the unconfined compressive strength (in MPa). The variability in the constants indicates the area specific nature of the correlations is affected by many factors such as: the smoothness of socket; regional rock mass properties; characteristics of concrete and its bond with the rock; and the models used to extrapolate the minimally mobilized side friction.

The preliminary design practice involves assignment of f_{\max} to all lithological units of the socket depending on the corresponding rock mass properties contrary to the fact that the amount of mobilized side resistance decreases with depth. Similarly, the contribution from end resistance is neglected as significant movement of pile end is required to mobilize end bearing (e.g. Williams et al. 1980; Carter and Kulhawy 1988).

The empirical models to predict f_{\max} are usually established based on results of load tests conducted on piles installed in certain geological formations and employing particular construction practices (e.g. Kulhawy et al. 2005). Utilizing these correlations for other geological formations and/or different construction practices may lead to unreliable prediction of the pile capacity, and requires careful assessment of the design by installing and testing test piles before design of production piles can be finalized. In many cases, time and cost constraints may not permit installation and testing of piles as part of the design procedure. Therefore, a predictive model for socket pile capacity that is derived based on the properties of the local rock formations and construction practices is necessary to facilitate safe and economic designs.

2 Objective and Scope of Work

The main objective of this study is to develop a model that is suitable for socketed piles installed in Dubai rock formations and construction procedures. The proposed model should reflect the behavior of rock

formations and construction practices prevalent in the Dubai area in particular and UAE in general. The average side resistance predicted by the model should also represent the true distribution of mobilized side resistance along the pile socket at serviceability limit state (i.e. at pile head movement to diameter ratio, $\delta^* < 1\%$). The model is developed based on analysis of the results from full scale pile-load tests conducted on five (5) reinforced concrete piles socketed in weak rock. The diameter of the test piles ranged from 0.9 to 1.5 m and the socket length varied from 10.2 to 15.4 m. Non-linear analysis is performed on the test data in order to develop the model to predict the average side resistance of the socket as a function of σ_c of the rock mass and the percentage relative movement at the top of the rock socket, $\delta^* = (\Delta_{TOP}/D) \times 100\%$ (where Δ_{top} is movement of top of socket). The developed nonlinear two-parameter model is verified by comparing its prediction with the experimental results.

3 Literature Review

UAE has been experiencing tremendous growth in construction of high rise structures during the last decade with concrete piles socketed into the rock as preferred foundation type. The overburden in many cases is either very shallow or absent; therefore, its contribution to the pile capacity is generally neglected. The preliminary evaluation of pile capacity is based on the estimate of socket capacity, which in most situations is obtained considering $f_{\max} - \sigma_c$ correlations. The pile capacity is often revised during the conceptual design stage after conducting preliminary pile load tests. In some situations, where no pile load testing is conducted, the cost of constructing piles following overly conservative design becomes significant. The preliminary design is usually conservative since f_{\max} is assigned to the entire socket length, which is contrary to observed load distribution pattern along the socket as limiting side resistance is not fully mobilized at all depth levels.

In addition, the end bearing is neglected in typical pile foundations in the UAE due to high length to diameter ratio of sockets. The large socket length is required to provide anchorage of high rise structures against uplift. Serviceability limit state often controls the design and end resistance is neglected due to its

limited mobilization (Kulhawy et al. 2005; Carrubba 1997; Rosenberg and Journeaux 1976; Pells 1999; Nam and Vipulanandan 2008; Seidel and Collingwood 2001).

Table 1 lists selected models from the literature based on functional form of Eq. (1). Rosenberg and Journeaux (1976) proposed a model to estimate f_{\max} based on six data points, with σ_c between 0.5 and 34 MPa. Horvath and Kenney (1979) reported 87 field tests conducted mostly in sedimentary rock with $\sigma_c \leq 0.4$ MPa, and they defined the capacity as the maximum applied test load. Horvath et al. (1983) subsequently discussed the effect of socket roughening on improving its shaft capacity, and proposed a method for evaluating the roughness and its effect on

the socket resistance. Their method considers factors such as socket radius, socket length and height of asperities. Meigh and Wolski (1979) compared the results for a number of loading tests with the predictions of the relationships proposed by Rosenberg and Journeaux (1976) and proposed a new relationship.

Rowe and Armitage (1984, 1987) summarized the design of socketed-piles in weak rock based on reviewing more than 60 load tests at different sites with σ_c ranging from 0.4 to 40 MPa. They subdivided the data into several roughness classes for socket as suggested by Pells et al. (1980) based on the depth and width of grooves. Carter and Kulhawy (1988) re-examined the same data and suggested a lower bound

Table 1 Selection of correlations for prediction of f_{\max} in literature

Relationship number	Reference	A	B
[1]	Rosenberg and Journeaux (1976)	0.375	0.515
[2]	Meigh and Wolski (1979)	0.219	0.6
[3]	Reynolds and Kaderabek (1980)	0.3	1.0
[4]	Williams et al. (1980)	0.435	0.37
[5]	Williams and Pells (1981) (best fit line with $r^2 = 1$)		
	(a) For $\sigma_c \leq 1$ MPa	0.506	0.159
	(b) For $1 \text{ MPa} \leq \sigma_c \leq 2.5$ MPa	0.512	0.3
	(c) For $2.5 \text{ MPa} \leq \sigma_c \leq 6$ MPa	0.422	0.495
[6]	Horvath et al. (1983)		
	(a) Lower bound	0.2	0.5
	(b) Upper bound	0.3	0.5
[7]	Rowe and Armitage (1987):		
	(a) Regular and clean socket	0.45	0.5
	(b) Rough socket	0.6	0.5
[8]	Carter and Kulhawy (1988)	0.2	0.5
[9]	Reese and O'Neill (1988)		
	(a) For $\sigma_c \leq 1.9$ MPa	0.15	1.0
	(b) For $\sigma_c > 1.9$ MPa	0.2	0.5
[10]	Kulhawy and Phoon (1993)		
	(a) Upper bound	0.675	0.5
	(b) Mean behavior	0.45	0.5
	(c) Lower bound	0.225	0.5
[11]	Zhang and Einstein (1998)		
	(a) Smooth socket	0.4	0.5
	(b) Rough socket	0.8	0.5
[12]	Ng et al. (2001) (granitic rock)	0.19	0.5
[13]	Prakoso (2002) (regression line with $r^2 = 0.51$ by Kulhawy et al. 2005)	0.47	0.7

model. Similarly, Zhang and Einstein (1998) examined published data (i.e. Rosenberg and Journeaux 1976; Meigh and Wolski 1979; Williams and Pells 1981; Horvath 1982; Kulhawy and Phoon 1993) and proposed relationships for smooth and rough sockets. Zhang and Einstein (1998) also proposed a relationship similar to that proposed by Carter and Kulhawy (1988).

Kulhawy and Phoon (1993) studied a large database of load tests reported by Rowe and Armitage (1984), Bloomquist and Townsend (1991), and McVay et al. (1992), and suggested a relationship representing the mean of the data (i.e. similar to Rowe and Armitage 1987).

Williams et al. (1980) suggested a model for predicting socket capacity based on 18 loading tests at different sites with σ_c ranging from 0.5 to 80 MPa. Subsequently, Williams and Pells (1981) proposed a similar model for piles socketed in weak rock. Reese and O'Neill (1988) suggested relationships similar to Carter and Kulhawy (1987) (first relationship for σ_c up to 1.9 MPa and second relationship for $\sigma_c > 1.9$ MPa).

Ng et al. (2001) reviewed published load test data (i.e. Leung 1996; Carrubba 1997; Walter et al. 1997; Horvath et al. 1983; Williams 1980; and Williams and Pells 1981) in addition to data from 13 loading tests they conducted, and proposed a model to predict capacity of piles socketed into granite considering $\delta^* = 1\%$. They suggested using a Displacement Index (DI) to evaluate the fully mobilized side resistance from various load tests in different rock types. A DI of A was suggested for fully mobilized value of f_{\max} when displacement reaches a minimum of 1% of socket diameter and the gradient of resistance-displacement relationship becomes < 30 kPa/mm at the end of the curve. A DI of B was suggested for displacement of at least 0.4% of the pile diameter with a gradient < 200 kPa/mm at the end of the curve. Similarly, DI index C is suggested when side resistance is slightly mobilized. Prakoso (2002) reviewed available loading test data and considered only those tests that reached failure to establish a correlation for the socket resistance with the rock mass strength.

4 Site Investigations and Geology

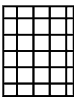
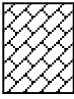
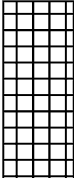
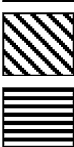


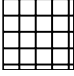
The test site is located approximately 20 km west of downtown Dubai. The site investigation involved 10 bore holes with depths ranging from 30 to 50 m, and the data was used to aid in design and installation of the test piles. The borings were advanced by using rotary drilling method with mud circulation. The subsurface geological conditions gleaned from the boreholes data show very few lateral variations and that the lithological units are primarily flat. The encountered bedrock formations were dominantly very weak and partially weathered Calcarenes, Calcareous gritty Sandstones/Calcarenes followed by the Calcirudites/conglomerates with interbeds of calcisiltites/siltstones up to end of boreholes. The RQD values ranged from 3 to 90%; however, more than 80% of the values ranged between 30 and 60% with close to very close spacing of fractures.

Table 2 presents the lithological units within the socket lengths at the locations of five (5) Test Piles (TP). Undisturbed core samples were obtained using double tube core barrel. The elastic modulus of the rock samples was determined from instrumented unconfined compression strength tests performed in accordance with ASTM D7012-14 (2014) and ASTM D4543-08 (2008). The site investigation also included 30 in situ High Pressure Dilatometer Tests (HPDT), which were conducted in three specified boreholes at specified intervals (about 2.0 m) using OYO Elastometer 2, with a pressure range of 0–20 MPa. The tests were carried out in accordance with the general guidelines of ASTM D4719-07 (2007).

5 Construction and Testing of Test Piles

The test piles (TP-1, TP-2, TP-3, TP-4, and TP-5) were installed and tested as a part of a project that included mixed use tower consisting of a high rise building comprising a hotel and residences and a stadium for aquatic performances. The preliminary design of the test piles was based on estimating f_{\max} following the procedure suggested by Williams and Pells (1981), with parameter β estimated from the correlations of mass factor with Rock Quality Designation (RQD) and fracture spacing. The construction of test piles involved surveying, installation of temporary casing, drilling, mechanical caliper logging, fabrication and

Table 2 Main lithological units encountered along the lengths of sockets

Test pile number	Depth (m)	Thick. (m)	Symbol	Description of rock	σ_c (MPa)
TP-1	0–0.65	0.65		Weak, light brown, fine grained calcarenite	4.71
	0.65–5.9	5.25		Very weak, light brown, fine grained calcarenite	2.04*
	5.9–8.15	2.25		Light brown siltstone	2.65
	8.15–15.4	7.25		Very weak reddish brown, conglomeratic siltstone	2.87*
TP-2	0–1.4	1.4		Very weak, light brown calcarenite	4.71
	1.4–2.8	1.4		1.68	
	2.8–2.95	0.15		1.57	
	2.95–6.6	3.65		Extremely weak brown, fine to medium grained calcarenite	0.87
	6.6–13.6	7.0		Very weak reddish brown, fine grained sandstone	3.02
	13.6–16.8	3.2		Very weak, reddish brown, conglomerate	2.91
TP-3	0–9.8	9.8		Very weak, light brown, fine grained calcarenite	4.3*
	9.8–12.8	3.0		Very weak, reddish brown, fine grained gypsiferous sandstone	2.45
TP-4	0–4.3	4.3		Very weak, light brown calcarenite	1.87
	4.3–8.8	4.5		Very weak, light brown, fine grained calcarenite	2.4*
	8.8–12.8	4.0		Very weak, reddish brown, conglomeratic siltstone	3.1
TP-5	0–1.2	1.2		Very weak, light brown, fine grained calcarenite	4.5*
	1.2–10.2	9.0			1.3*

*Average value for two or more rock samples within that specific depth

installation of steel cage, concreting, and extraction of temporary casing. Two piles had diameter, $D = 1.5$ m and socket length, $L = 15.4$ m; two piles had $D = 1.2$ m and $L = 12.4$ m and one pile had $D = 0.9$ m and $L = 10.2$ m. The compressive strength and elastic modulus of the concrete used to construct the piles were determined from compressive loading tests conducted on cylindrical specimens from the same patches used for piles construction. The piles geometry and their concrete properties are provided in Table 3. The integrity of the test piles was checked by cross-hole sonic logging using four (4) preinstalled water tight ducts. Ceramic transducers along with the cross-hole analyzer manufactured by Sonitek were

used to examine the integrity of concrete and the test piles. The sonic logging was carried out after 7–12 days of casting the concrete.

5.1 Pile Instrumentation

A pair of tell-tale rods was installed in each pile with hydraulic cell assembly to monitor the movement against a reference frame. Tokyo Sokki Model SDP-100C 100 mm maximum stroke resistance-type displacement transducers were used to monitor and record displacement of test piles. Vibrating wire rebar strain gauges of the type Geokon-4911 were installed at three levels (SG-1, SG-2, and SG-3) along the

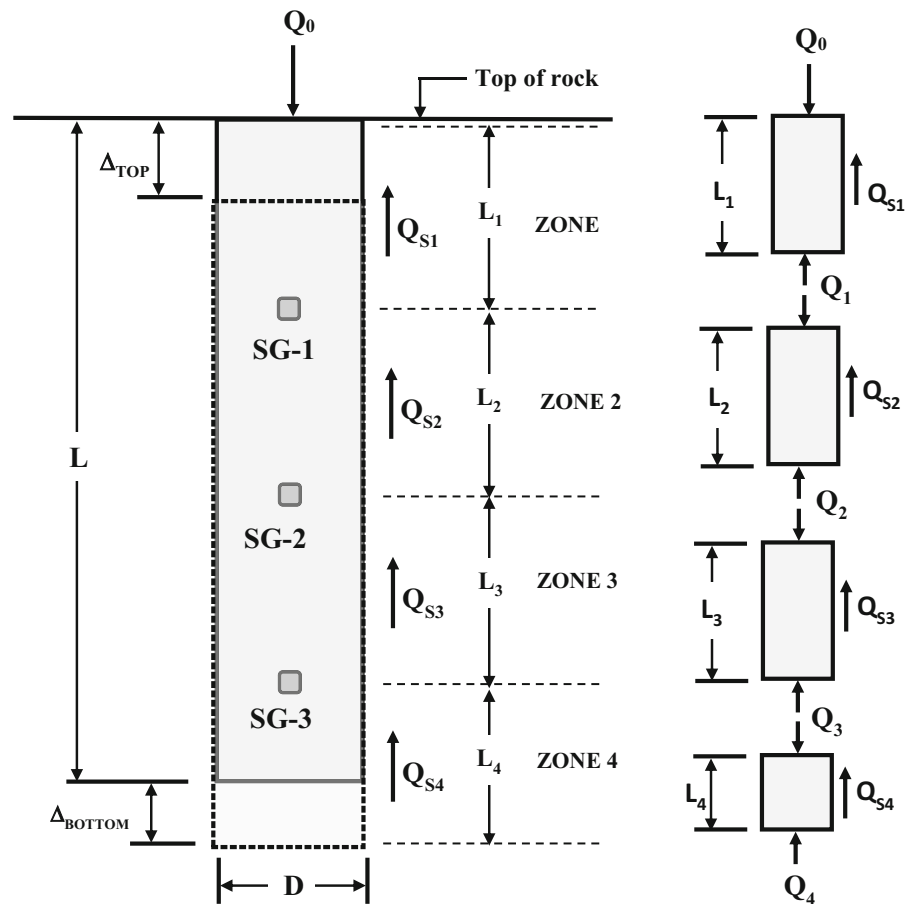
Table 3 Pile configurations, instrumentation, and loading stages

Test pile number	D (m)	L (m)	Pile modulus (MPa)	$\bar{\sigma}_c$ (MPa)	Depth (m)			Load stages (MN)
					SG-1	SG-2	SG-3	
TP-1	1.5	15.4	34.3	2.7	4.8	9.6	14.4	5.5, 11, 16.5, 22, 27.5, 33
TP-2	1.5	15.4	34.3	2.3	4.8	9.6	14.4	
TP-3	1.2	12.8	37.1	3.9	4.0	8.0	11.8	3.5, 7, 10.6, 14.1, 17.7, 21.1
TP-4	1.2	12.8	37.1	2.5	4.0	8.0	11.8	
TP-5	0.9	10.2	38.5	1.6	3.0	6.0	9.2	2, 4, 6, 8, 10, 12

socket with four (4) units at each level. The depths of the strain gauge levels for the different test piles are listed in Table 3 as well. Moreover, the test piles were fitted with pressure transducers of vibrating wire type (Geokon Model 4500HH-10,000). Figure 1 shows the schematic diagram of locations of strain gauge levels (SG-1, SG-2 and SG-3), which were used for calculating the frictional resistance values at the pile/rock

interface for different zones along the socket length. The average compressive strength of rock along the socket length ($\bar{\sigma}_c$) determined from unconfined compressive strength testing of the relevant undisturbed rock samples for the five test piles are summarized in Table 3.

Fig. 1 Generalized location of strain gauge levels and zones of load transfer



5.2 Load Test Procedure and Loading Setup

The pile load tests were conducted according to ASTM D1143-13 (2013). The maximum estimated applied load for the tests was based on limiting the compressive stresses in piles to 35% of 28-day cube strength of concrete (50 MPa) or settlement of pile head by 1% of the diameter whichever governs. Each pile was loaded in six increments, each of 15–20% of the maximum applied test load. Each increment was maintained for a period of not less than 4 h and movement of the pile top (Δ_{TOP}) and the strain gage measurements were recorded at 1 min intervals at each loading stage for each test pile. The deflection of the test pile was calculated based on the strain measurements along the pile length. Movement of the pile bottom (Δ_{BOTTOM}) is then calculated from the

difference between the pile top movement and the pile deflection. Figures 2, 3 and 4 present typical results of deflection of pile top and bottom (calculated) versus load at all six load increment stages for all test piles. The loads shown on Figs. 2, 3 and 4 are the loads applied at the pile heads.

6 Interpretation of Load Tests and Regression Model

The strain gauge readings were used to establish the load distribution along the socket. The net loads at the pile/rock interface along different zones (i.e. Q_{S1} , Q_{S2} , Q_{S3} and Q_{S4}) and the distribution of the internal load (i.e., loads at the bottom of each zone— Q_1 , Q_2 , Q_3 and Q_4) along the socket length are determined at each

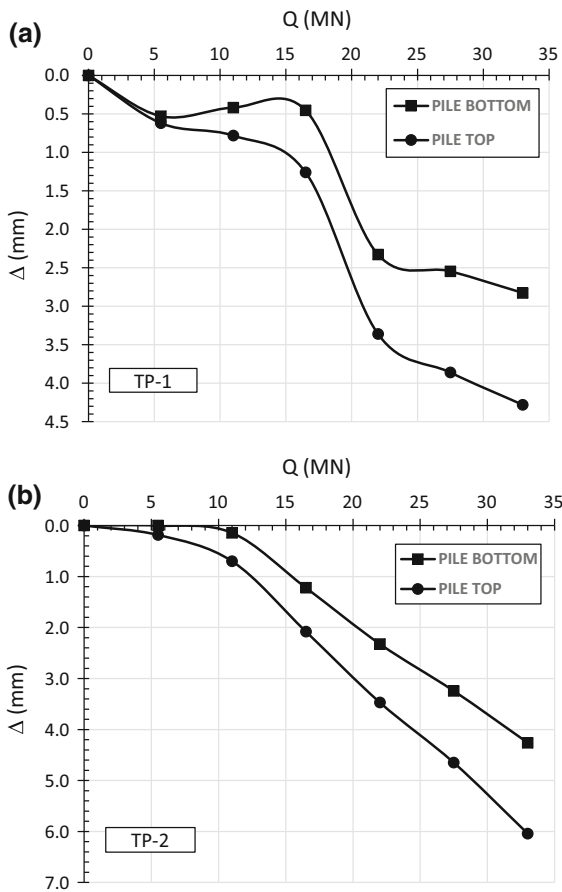


Fig. 2 Movement of pile top and calculated movement of pile bottom (socket length = 15.4 m, diameter = 1500 mm). **a** TP-1 and **b** TP-2

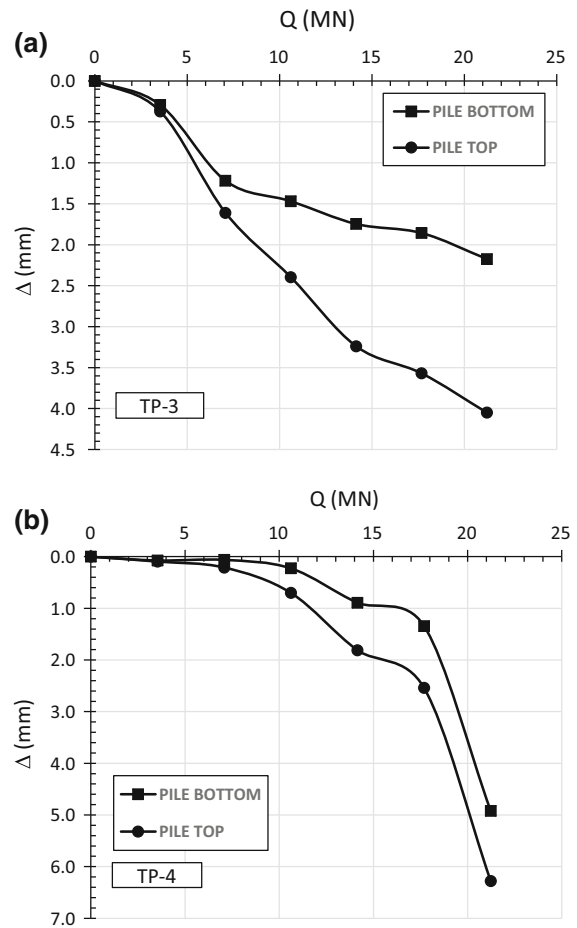


Fig. 3 Movement of pile top and calculated movement of pile bottom (socket length = 12.8 m, diameter = 1200 mm). **a** TP-3 and **b** TP-4

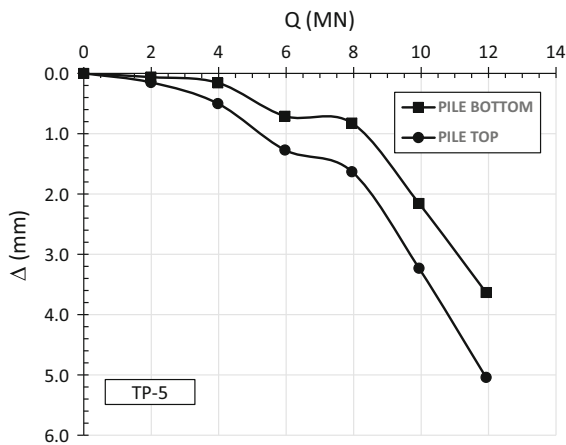


Fig. 4 Movement of pile top and calculated movement of pile bottom (socket length = 10.2 m, diameter = 900 mm)

loading stage by satisfying compatibility and equilibrium equations for each individual zone. The compatibility equation is used for zone i to determine Q_i ($i = 1-4$) which depends on the measured strain (ε), cross-sectional area of the pile (A_p) and elastic modulus of the pile (E_p). Q_i is calculated as,

$$Q_i = \left[\frac{\varepsilon_i}{1 - \varepsilon_i} \right] (A_p E_p) \quad (2)$$

Considering equilibrium in the vertical direction for each zone, Q_{Si} is then determined using the following equation:

$$Q_{Si} = Q_0 - Q_i \quad (3)$$

The applied load at the top of zone 1 is Q_0 , which is taken as the applied load at pile head. In addition, the base reaction (Q_4) or the load at the bottom of zone 4 is ignored to render the problem determinant considering that the displacements of test piles are relatively small (less than 8 mm). This is justified because most of the applied load is transferred to the sides of zones 1, 2, and 3 and the length of zone 4 is relatively small compared to the rock socket (6–10% of the rock socket). Yildirim (2009), among many other researchers, reported that the entire load for rock-socketed piles is supported by side resistance when the displacement is less than 10 mm. Furthermore, considering the maximum displacement achieved in all pile load tests, the maximum calculated toe movement was less than 0.4% of the pile diameter, which is considered insufficient to mobilize noticeable end bearing resistance.

Table 4 summarizes the calculated percentages of the load transfer to the sides at the final loading stage as an example. The percentages of the loads transferred to zone 4 are insignificant (e.g., < 8% at the final loading stage for TP-3) for all test piles. It can be inferred from Table 4 that more than 92% of the applied load (Q_0) has already been transferred to the pile/rock interface (sum of zones 1, 2, and 3) considering the compatibility and equilibrium of zones above zone 4.

The net loads (Q_{Si}) at the pile/rock interface for each zone were then divided by the respective surface areas to determine the side resistances (f_1, f_2, f_3 and f_4), which were then averaged (weighted f_{avg}) for the entire length of the rock socket. Figure 5 shows the distribution of unit side resistances and average unit side resistances at some selected loading stages for TP-1. The representation of distribution of side resistance by an average value reflect the true nature of load distribution along the socket and accurately predicts the capacity at corresponding movement of the pile head.

6.1 Development of Nonlinear Regression for Prediction of Socket Capacity

A non-linear regression analysis was conducted to develop a model that describes the relationship between the socket side resistance and the rock mass strength utilizing the load tests results along with the measured rock compressive strength. The test results used in developing the model consisted of average side resistances and the corresponding pile top movement for each test pile at each loading stage as shown in Fig. 6. This regression analysis established the relationship between the average socket side resistance (f_{avg}), the corresponding rock compressive strength (σ_c) and the percentage of pile movement at the top of socket relative to the pile diameter (δ^* %) through a multiple nonlinear power model. This relationship is obtained in the following form:

$$f_{avg} = \alpha (\delta^*)^\beta (\sigma_c)^\gamma \quad (4)$$

where $\delta^* = (\Delta_{TOP}/D) \times 100\%$ and α , β , and γ are parameters to be determined. Initially, the Levenberg–Marquardt algorithm (LMA) is used to perform the curve fitting procedure by minimizing the sum of the squares of the residuals. The LMA solution for the

Table 4 Percent of Q_0 transferred to the sides (Q_s/Q_0) for each zone (final loading stage)

Pile No	Zone 1	Zone 2	Zone 3	Zones 1 + 2 + 3	Zone 4
TP-1	55.4	35.6	7.2	98.2	1.8
TP-2	52.2	31.5	12.3	96.0	4.0
TP-3	41.7	31.4	19.0	92.1	7.9
TP-4	57.7	23.5	12.5	93.7	6.3
TP-5	37.7	35.4	20.1	93.2	6.8

Fig. 5 Typical development of unit side resistance at four selected loading stages (TP-1)

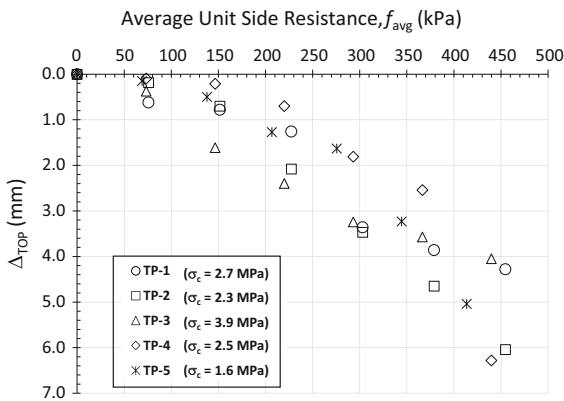
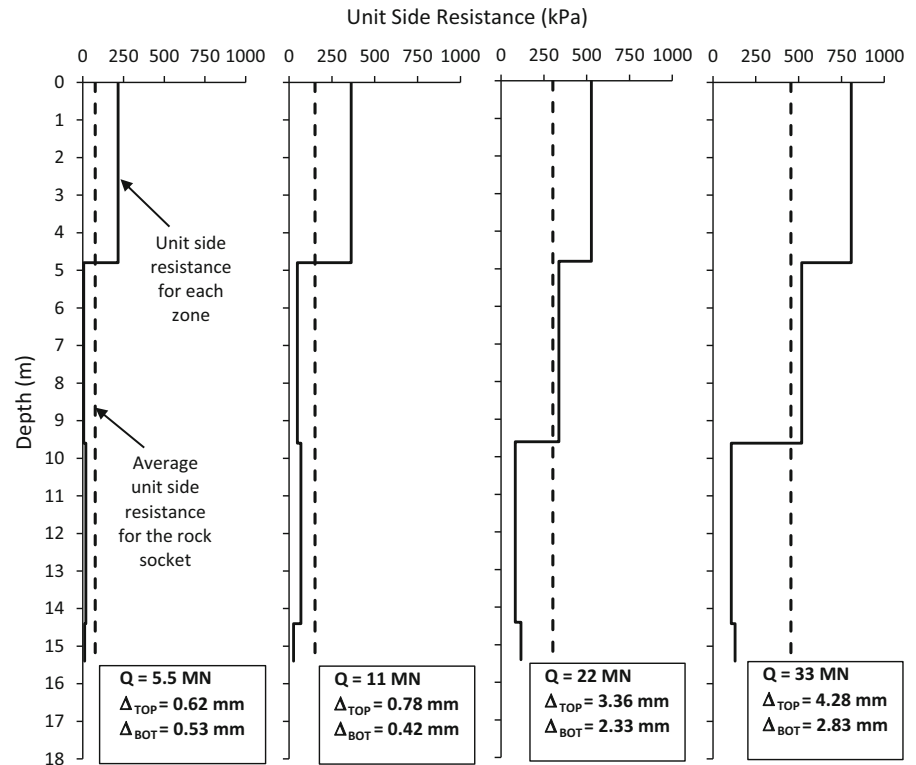


Fig. 6 Average unit side resistances of all test piles for model analysis

unknown parameters provided excellent fit for the data with $r^2 = 0.93$ and with reasonably low standard errors for each estimate. The obtained estimates for the parameters are rounded for convenience which reduced r^2 to 0.92 as shown in Fig. 7. The functional form of the proposed model representing the average side resistance (in MPa) for piles socketed in very weak to weak rocks of Dubai area is given by:

$$f_{avg} = 0.56 \times (\delta^*)^{0.6} \times (\sigma_c)^{0.4} \tag{5}$$

In a standard dimensionless form, the relationship can be rewritten as:

$$\left(\frac{f_{avg}}{p_a}\right) = 2.212 \times (\delta^*)^{0.6} \times \left(\frac{\sigma_c}{p_a}\right)^{0.4} \tag{6}$$

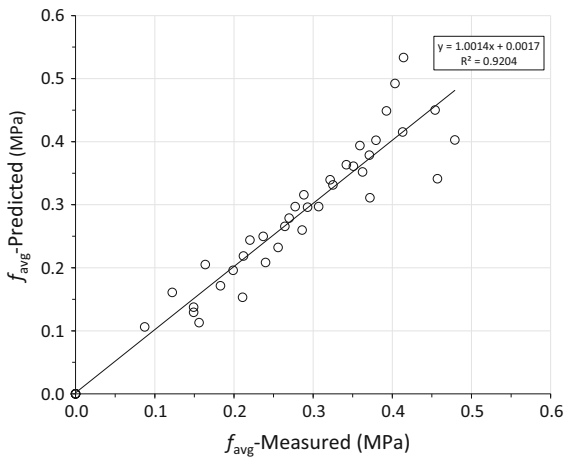


Fig. 7 Predictions of proposed model compared with all measured values

where p_a is the atmospheric pressure in the desired units (1 atm = 101.3 kPa = 14.7 psi = 1.058 tsf). Figure 8 compares the predictions of the proposed model (Eq. 5) with the measured values from the load test on test pile TP-2. Regression models based on other rock parameters such as RQD and Elastic moduli were also considered; however, regression model based on compressive strength and pile head movement yielded the best fit.

7 Evaluation of Performance of Developed Model

The performance of the developed model is evaluated through comparison with measured side friction as

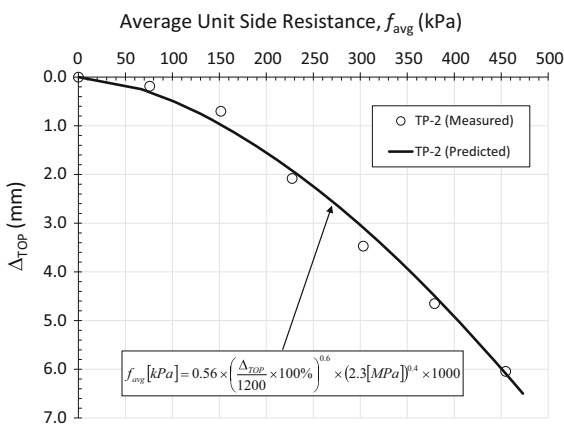


Fig. 8 Model prediction of f_{avg} in the socket compared with the measured f_{avg} for TP-2

well as predictions of other models available in the literature. Figure 9 presents the comparison of proposed model with the models presented in Table 1. The range of unconfined compressive strength value from 0.5 to 5 MPa is considered for the comparison. For intermediate geomaterials such as very soft rock or hard soil, σ_c usually ranges from 0.4 to 2.0 MPa (Seidel and Haberfield 1995). The proposed model which calculates f_{avg} of the socket is plotted for four selected values of δ^* (0.4, 0.6, 0.9 and 1.5%). This range (0.4–1.5%) was selected based on reviewing published criteria of limit displacements (Table 5) required to fully or significantly mobilize side resistance ($\approx f_{max}$). Figure 9 shows significant scatter of the predictions using selected relationships available in the literature, which can be attributed to many factors indicating site or area specific nature of the models. The factors that affect f_{max} can range from concrete characteristics (bond strength, asperities, etc.), socket length and properties (smoothness), type of drilling fluid used in construction (polymer based versus mineral), specific characteristics of geological formation, and models used to extrapolate side resistance to its maximum or limiting value.

The qualitative discussion on the performance of the proposed model in comparison with other models available in the literature is based on the assumption that full mobilization of side resistance in upper zones of socket will occur when the pile movement at the top of rock socket ranges from $\delta^* = 0.6\text{--}0.9\%$. This range of δ^* is considered practical and agreeable with the findings of Ng et al. (2001) among many others.

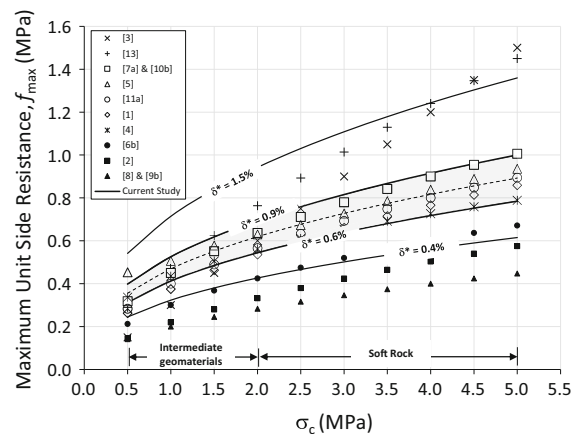


Fig. 9 Comparison of selected models based on f_{max} with the proposed model based on f_{avg}

Table 5 Summary of f_{max} and corresponding limit displacements by various researchers

Reference	Approximate limit displacement (mm)	δ^* (%)
Horvath and Kenney (1979)	6	0.5–1.5
Ng et al. (2001)	4–10	0.4–1.4
Williams et al. (1980)	6	0.9
Rosenberg and Journeaux (1976)	6.35	–
NCHRP (2006)	5–10	–
Basarkar and Dewaikar (2006)	10	–
Akguner and Kirkit (2012) (TP-3)	6.6	0.825
Carrubba (1997) (TP-1)	7	0.5833

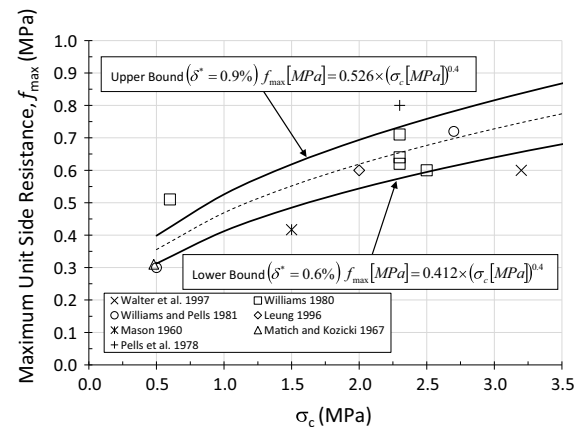


Fig. 10 Comparison of the proposed model with published values of measured f_{max}

Table 6 Selection of limiting value of side resistance from literature

Test pile number	Reference	D (m)	Rock Type	σ_c (MPa)	Reported f_{max} (MPa)
1	Walter et al. (1997)	0.9	Mudstone	3.2	0.60
2	Williams et al. (1980)	1.12	Mudstone	0.6	0.51
3	Williams et al. (1980)	1.22	Mudstone	2.5	0.60
4	Williams et al. (1980)	1.30	Mudstone	2.5	0.64
5	Williams et al. (1980)	1.23	Mudstone	2.3	0.71
6	Williams et al. (1980)	1.35	Mudstone	2.3	0.62
7	Matich and Kozicki (1967)	0.61	Shale	0.48	0.31
8	Williams and Pells (1981)	0.66	Shale	0.5	0.30
9	Williams and Pells (1981)	0.79	Shale	2.7	0.72
10	Leung (1996)	–	Granite	2.0	0.60
11	Mason (1960)	0.61	Shale	1.5	0.42
12	Pells et al. (1978)	1.09	Mudstone	2.3	0.80

Figure 9 indicates that relationships 2, 8 and 9 significantly underestimate the maximum side resistance. The side shear is slightly mobilized when δ^* is less than 0.4% for relationships 2, 8 and 9 and less than 0.5% for relationship 6. On the other hand, the predictions of the majority of relationships (1, 4, 5, 7, 10 and 11) agree well with the predictions of the proposed model for δ^* ranging from 0.6–0.9%.

Figure 10 compares the predictions of the proposed model with the reported values of f_{max} in the literature for similar rocks, which were estimated to occur for δ^* ranging from 0.6–0.9%, and Table 6 provides a summary of these values of f_{max} . As can be noted from Fig. 10 and Table 6, one-third of f_{max} values are in good agreement with the mean of predicted values using the proposed model with $\delta^* = 0.75\%$, 25% of the data agrees with the lower bound of the proposed model prediction for $\delta^* = 0.6\%$ and approximately 10% is close to the upper bound ($\delta^* = 0.9\%$). The remaining one-third values are either slightly above or below the bounds. This comparison indicates that the displacement ratio range ($0.6\% \leq \delta^* \leq 0.9\%$) is representative of significant mobilization of side friction (Fig. 11).

8 Conclusions

This article presents the results of five (5) instrumented load tests on concrete piles socketed in rock formations of Dubai area. Three (3) different pile diameters (0.9, 1.2 and 1.5 m) with sockets having

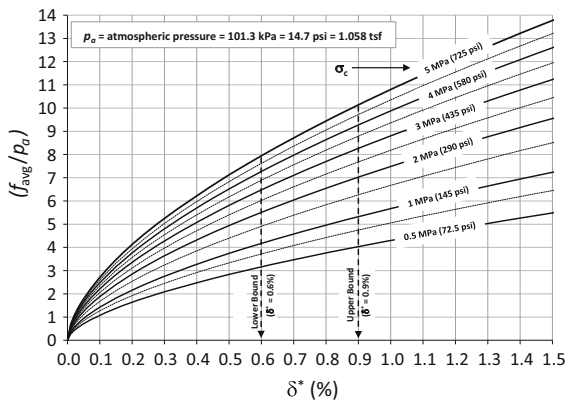


Fig. 11 Design chart to estimate the f_{avg} of a rock socket based on the proposed model

length-to-diameter ratio of more than 10 are tested and analyzed. A two parameter model is proposed to better predict the socket capacity as a function of σ_c and δ^* for preliminary design stage and sizing of preliminary test piles if required. The main conclusions from the study can be summarized as follows.

1. The measured movement of pile head ranges from approximately 4 to > 6 mm; whereas, calculated movement of the pile end ranges from 2 to 4 mm.
2. The maximum calculated load transferred to the pile toe was less than 8% of the test load indicating negligible mobilization of end bearing.
3. The developed model predicted the results of load tests conducted as part of this study with high accuracy. In addition, the predicted f_{avg} values seem to better represent the true distribution of side resistance along the length of socket.
4. Limiting values of the side resistance will mobilize for δ^* ranging from 0.6 to 0.9%, which is also the serviceability limit criteria in Dubai area.
5. Comparing the predictions of the proposed model with the predictions of other relationships available in the literature indicates wide variation, which suggests the area specific nature of these relationships. Meanwhile, approximately half to two-thirds of these relationships predicted f_{max} to occur at $0.6\% \leq \delta^* \leq 0.9\%$.

Acknowledgements The authors extend their gratitude to the Office of Graduate Studies and Research at the American University of Sharjah, technical staff of DEC Dubai, and Aqeel Ahmad of the American University of Sharjah for their support in testing and analysis of the test piles.

References

- Akguner C, Kirkit M (2012) Axial bearing capacity of socketed single cast-in-place piles. *Soils Found* 52(1):59–68
- ASTM D1143-13 (2013) Standard test methods for deep foundations under static axial compressive load. ASTM International, West Conshohocken, PA. www.astm.org
- ASTM D4719-07 (2007) Standard test methods for prebored pressuremeter testing in soils (withdrawn 2016). ASTM International, West Conshohocken, PA. www.astm.org
- ASTM D4543-08 (2008) Standard test methods for prebored pressuremeter testing in soils. ASTM International, West Conshohocken, PA. www.astm.org
- ASTM D7012-14 (2014) Standard test method for compressive strength and elastic moduli of intact rock core specimens under varying states of stress and temperatures. ASTM International, West Conshohocken, PA. www.astm.org
- Basarkar SS, Dewaikar DM (2006) Load transfer characteristics of socketed piles in Mumbai region. *Soils Found* 46(2):247–257
- Bloomquist D, Townsend F (1991) Development of in situ equipment for capacity determination of deep foundations in Florida limestone. Report to Florida Department of Transportation, University of Florida, Gainesville
- Bouafia A (2003) Load settlement behavior of socketed piles in sandstone. *Geotech Geol Eng* 21(4):389–398
- Carrubba P (1997) Skin friction of large-diameter piles socketed into rock. *Can Geotech J* 34:230–240
- Carter JP, Kulhawy FH (1987) Analysis and design of foundations socketed into rock. Res. Rep. 1493-4, Geotechnical Engineering Group, Cornell University, Ithaca, New York
- Carter JP, Kulhawy FH (1988) Analysis and design of drilled shaft foundations socketed into rock. Report el-5918. Electric Power Research Institute, Palo Alto
- Horvath RG (1982) Drilled piers socketed into weak shale-methods of improving performance. PhD Dissertation, University of Toronto
- Horvath RG, Kenney TC (1979) Shaft resistance of rock-socketed drilled piers. In: Proceedings of the symposium on deep foundation, ASCE, New York, pp 182–214
- Horvath RG, Kenney TC, Kozicki P (1983) Methods of improving the performance of drilled piers in weak rock. *Can Geotech J* 20:758–772
- Kulhawy FH, Phoon KK (1993) Drilled shaft side resistance in clay soil to rock. In: Proceedings of design and performance of deep foundations: piles and piers in soil and soft rock, Geotechnical. Special Publication No. 38, ASCE, New York, pp 172–183
- Kulhawy FH, Prakoso WA, Akbas SO (2005) Evaluation of capacity of rock foundation sockets. In: G Chen et al (eds) Proceedings of the 40th U.S. Symposium on Rock Mechanics, Anchorage, Alaska, paper 05-767
- Leung CF (1996) Case studies of rock-socketed piles. *Geotechnical Engineering, Bangkok*
- Mason RC (1960) Transmission of high loads to primary foundations by large diameter shafts. In: Proceedings of ASCE convention, ASCE, New York
- Matic MA, Kozicki P (1967) Some load tests on drilled cast-in-place concrete caissons. *Can Geotech J* 4:367–375

- McVay MC, Townsend FC, Williams RC (1992) Design of socketed drilled shafts in limestone. *J Geotech Eng* 118(10):1626–1637
- Meigh AC, Wolski W (1979) Design parameters for weak rocks. In: *Proceedings of 7th European conference on SMFE*, vol 5, Brighton
- Nam MS, Vipulanandan C (2008) Roughness and unit side resistances of drilled shafts socketed in clay shale and limestone. *J Geotech Geoenviron Eng* 134(9):1272–1279
- NCHRP Transportation Research Board (2006) NCHRP SYNTHESIS 360 rock-socketed shafts for highway structure foundations. NCHRP, Washington
- Ng C, Yau T, Li J, Tang W (2001) Side resistance of large diameter bored piles socketed into decomposed rocks. *J Geotech Geoenviron Eng* 127:642–657
- Omer JR, Robinson RB, Delpak R, Shih JKC (2003) Large scale pile tests in Mercia Mudstone: data analysis and evaluation of current design method. *Geotech Geol Eng* 21(3):167–200
- Pells PJ (1999) State of practice for the design of socketed piles in rock. In: *Proceedings of the 8th Australia New Zealand conference on geomechanics*, Australian Geomechanics Society, pp 307–327
- Pells OJ, Douglas DJ, Rodway B, Thorne C, McManhon BK (1978) Design loadings for foundations on shale and sandstone in the Sydney region. Res Rep No R315, University of Sydney, Sydney
- Pells PJ, Rowe RK, Turner RM (1980) An experimental investigation into side shear for socketed piles in sandstone. In: *Proceedings of the International Conference on Structural Foundations on Rock*, vol 1, pp 291–302
- Prakoso WA (2002) Reliability-based design of foundations in rock mass. PhD dissertation. Cornell University
- Reese LC, O'Neill MW (1988) Drilled shafts: construction procedures and design methods. Publication No. FHWA-HI-88-042, Federal Highway Administration, Washington, DC
- Reynolds RT, Kaderabek TJ (1980) Miami limestone foundation design and construction. ASCE, New York
- Rosenberg P, Journeaux NL (1976) Friction and end bearing tests on bedrock for high capacity socket design. *Can Geotech J* 13:324–333
- Rowe RK, Armitage HH (1984) Design of piles socketed into weak rock. Report GEOT-11-84. University of Western Ontario
- Rowe RK, Armitage HH (1987) A design method for drilled piers in soft rock. *Can Geotech J* 24:126–142
- Seidel JP, Collingwood B (2001) A new socket roughness factor for prediction of rock socket shaft resistance. *Can Geotech J* 38:138–153
- Seidel JP, Haberfield CM (1995) The axial capacity of pile sockets in rocks and hard soils. *Ground Eng* 28(2):33–38
- Walter D, Burwash WJ, Montgomery RA (1997) Design of large-diameter drilled shafts for Northumberland Strait bridge project. *Can Geotech J* 34:580–587
- Williams AF (1980) The design and performance of piles socketed into weak rock. PhD Dissertation, Monash University
- Williams AF, Pells PJ (1981) Side resistance rock sockets in sandstone, mudstone, and shale. *Can Geotech J* 18:502–513
- Williams AF, Johnston IW, Donald IB (1980) The design of socketed piles in weak rock. In: *Proceedings of the International Conference on Structural Foundations on Rock*, pp 327–347
- Yildirim S (2009) Site investigations and foundation design. Birsen Yayinevi, Istanbul
- Zhang L, Einstein HH (1998) End bearing capacity of drilled shafts in rock. *J Geotech Geoenviron Eng* 124(7):574–584